www.czasopisma.pan.pl PAN POLSKA AKADEMIA NAUK www.journals.pan.pl

ARCHIVES OF ELECTRICAL ENGINEERING VOL. 61(3), pp. 373-388 (2012)

DOI 10.2478/v10171-012-0030-2

Modified algorithms of direct power control of AC/DC converter co-operating with the grid

KRZYSZTOF KULIKOWSKI

Department of Power Electronics and Electric Drivers
Bialystok University of Technology
Bialystok, Poland
e-mail: k.kulikowski@pb.edu.pl

(Received: 11.01.2012, revised: 19.03.2012)

Abstract. This paper briefly describes direct power control methods for two- and three-level AC/DC converters and their modified DPC 3×2-δ and the DPC 5×2-δ algorithms. It also presents two new control methods DPC-3Am (direct power control 3 areas with modification) and the DPC-3L-3Am (direct power control 3 levels 3 areas with modification). The research results were used to compare the described methods. The comparison was based on an average value of switching frequency and current distortion coefficient. Experimental investigations into the methods have shown that the use of the modified DPC methods reduces the number of switchings by more than 70% compared with the standard DPC method.

Key words: DPC, optimization of DPC method, three-level converter, nonlinear control

1. Introduction

Very often the quality of control methods for the AC/DC converter involve quantification of the coefficient of current deformations, however the converter's efficiency is often neglected although it has a significant impact on the operation costs of the converter as well as on the size of cooling system. The efficiency of the device depends only on a control method selected for a specific converter (with fixed parameters of used semiconductors) and a specific work point. This is caused by the influence of the chosen methods on an average switching frequency of the converter. Owing to a possibility of direct control of semiconductor switches, the DPC methods [1-3] are perfectly suited to optimize the number of switchings in order to reduce switching power losses.

The paper contains the results of experimental investigations of the described modified DPC methods of three- and two-level AC/DC converters.

www.czasopisma.pan.pl PAN POLSKA AKADEMIA NAUK www.journals.pan.pl

2. Mathematical model of the converter

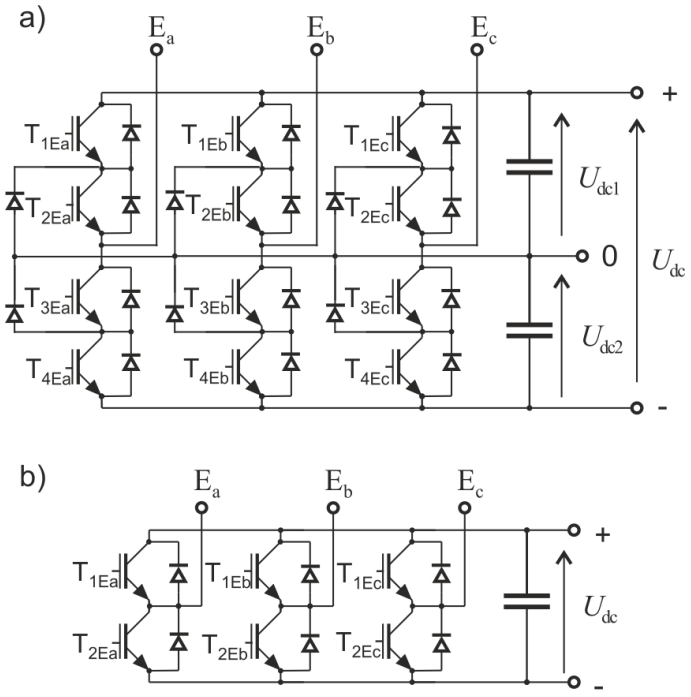

Fig. 1. Configuration of three-level (a) and two-level (b) converters

The relationships (1) and (2) [7] describe the input voltage vectors of the converter in $\alpha\beta$ stationary reference frame with respect to three- and two-level configuration [4, 5]:

$$\mathbf{U_d}[n] = \begin{cases} \frac{2}{3}U_{dc} \cdot e^{j(n-21)\frac{\pi}{3}}, \text{for } n = \{21, 22..., 26\}, \\ \frac{\sqrt{3}}{3}U_{dc} \cdot e^{j(n-15)\frac{\pi}{3}+\frac{\pi}{6}}, \text{for } n = \{15, 16..., 20\}, \\ \frac{1}{3}U_{dc} \cdot e^{j(n-3)\frac{\pi}{3}}, \text{for } n = \{3, 4,..., 14\}, \\ \text{"}\mathbf{0}\text{"}, \text{for } n = \{0, 1, 2\}, \end{cases} \tag{1}$$

$$\mathbf{U_d}[n] = \begin{cases} \frac{2}{3}U_{dc} \cdot e^{j(n-1)\frac{\pi}{3}}, \text{for } n = \{1, 2..., 6\}, \\ \text{"}\mathbf{0}\text{"}, \text{for } n = \{0, 7\}, \end{cases} \tag{2}$$

where: U_{dc} – DC link voltage, "**0**" – zero vector, n – vector number.

www.czasopisma.pan.pl PAN POLSKA AKADEMIA NAUK www.journals.pan.pl

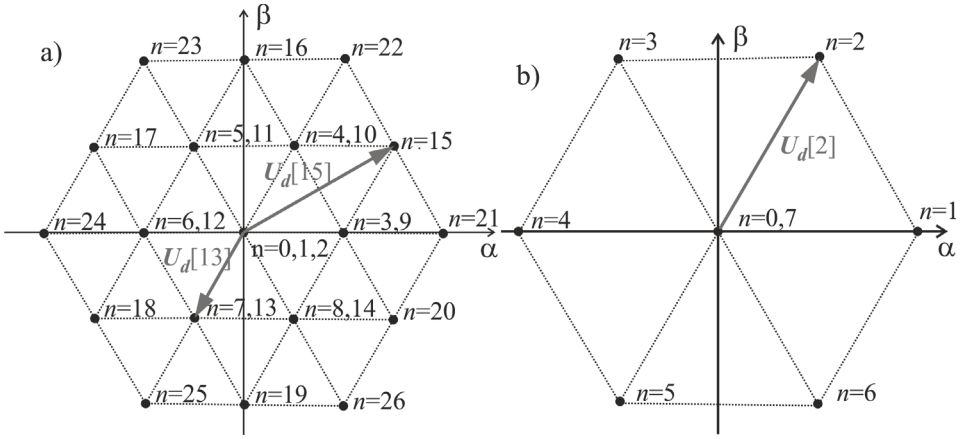

Fig. 2. Graphical interpretation of converter voltage vectors for three-level (a) and two-level (b) converters

Vectors of current derivative of AC/DC converter

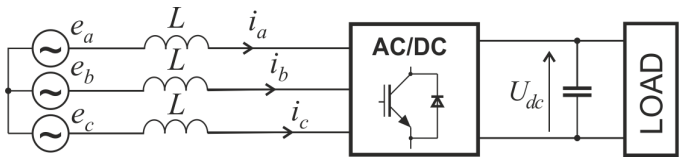

Fig. 3. Schematic diagram of AC/DC converter

The AC/DC converter shown in Figure 3 can be described by relationship (3) in *xy* rotating reference frame (3) [6]:

$$\mathbf{E} = L\frac{d}{dt}\mathbf{I_{xy}} + j\omega_1 L\mathbf{I_{xy}} + \mathbf{U_d}[n]\cdot e^{-j\omega_1 t}, \tag{3}$$

where: $\mathbf{I}_{xy}$ – vector of current in xy rotating reference frame, L – inductance between the grid and the converter, $\mathbf{E}$ – grid voltage vector, ω_1 – grid angular frequency.

Equation (4) results from the transformation of Equation (3). The obtained voltage vector (Fig. 4a) is proportional to the vector of current derivative (Fig. 4b) that determines both the direction and speed of current changes:

$$L\frac{d}{dt}\mathbf{I_{xy}} = \mathbf{D}_u[n] = \mathbf{E} - j\omega_1 L\mathbf{I_{xy}} - \mathbf{U_d}[n]\cdot e^{-j\omega_1 t}, \tag{4}$$

where: $\mathbf{D}_u[n]$ – vector proportional to the vector of current derivative for the n-th converter voltage vector.

Graphic representation of formula (4) for two-level converter is shown in Figure 4.

www.czasopisma.pan.pl PAN POLSKA AKADEMIA NAUK www.journals.pan.pl

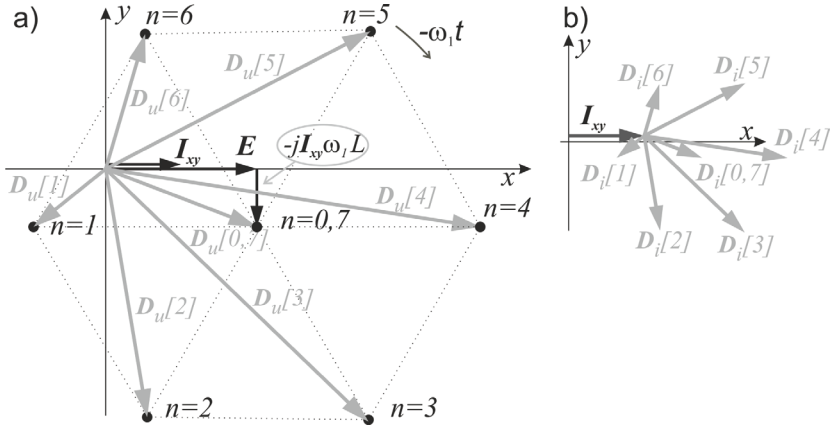

Fig. 4. Graphic representation of vectors proportional to vectors of current derivatives $\mathbf{D}_u[n]$ (a) and vectors of current derivatives $\mathbf{D}_i[n]$ (b)

3. Description of control methods

DPC 3×2

The DPC 3×2 [4] method makes it possible to control of the two current vector components by selecting voltage vector $\mathbf{U}_d[n]$ from the voltage vector selection table (Tab. 1). The choice depends on sector N as well as the current comparator states. The selection of sector N is determined by the angle of virtual flux vector $\mathbf{\Psi}_w$. The DPC method assumes that the virtual flux vector is delayed with respect to the grid voltage vector $\mathbf{E}$ by approximately $\pi/2$ (Fig. 6).

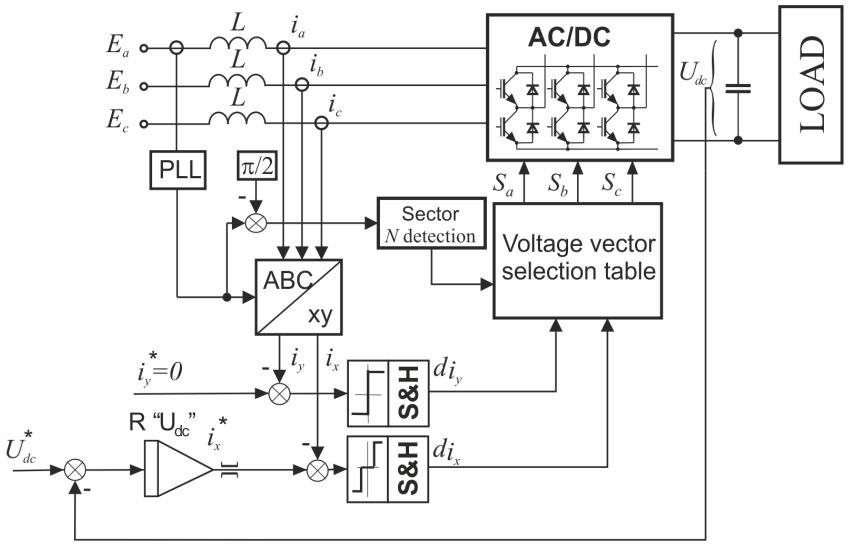

Fig. 5. Schematic diagram of DPC 3×2 method

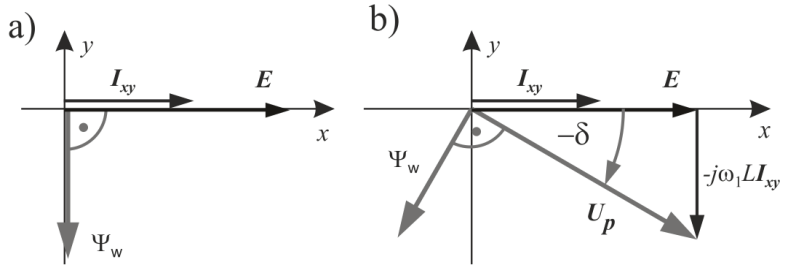

Fig. 6. Graphic interpretation of virtual flux vector for both DPC 3×2 (a) and DPC $3\times2-\delta$ (b) methods

Table 1. Voltage vector selection table for both DPC 3×2 and DPC $3\times2-\delta$ metods

		$N=1$	$N=2$	$N=3$	$N=4$	$N=5$	$N=6$
		number of voltage vector n					
$d_y=1$	$d_x=1$	5	6	1	2	3	4
	$d_x=0$	4	5	6	1	2	3
	$d_x=-1$	3	4	5	6	1	2
$d_y=-1$	$d_x=1$	6	1	2	3	4	5
	$d_x=0$	1	2	3	4	5	6
	$d_x=-1$	2	3	4	5	6	1

DPC $3\times2-\boldsymbol{\delta}$

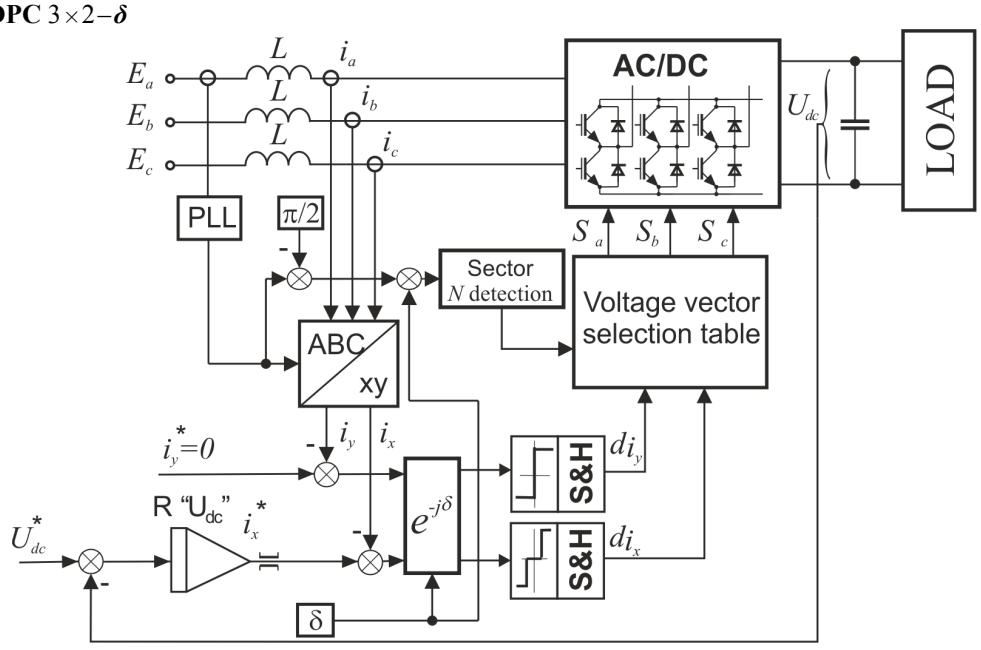

Fig. 7. Schematic diagram of DPC $3\times2-\delta$ method

The DPC 3×2 method does not take into account the voltage drop caused by current flow through inductors, which results in voltage shift on the converter feeder clamps with respect to

www.czasopisma.pan.pl PAN POLSKA AKADEMIA NAUK www.journals.pan.pl

the grid voltage vector **E** by angle δ (5). The vector of converter input voltage has also larger amplitude (see Fig. 6).

$$\delta = arctg\left(\frac{\omega L I_x}{|\mathbf{E}| + \omega L I_y}\right). \tag{5}$$

The shift between these voltage vectors may also cause an incorrect sector selection and, in consequence, deteriorate the quality of control. To minimize this negative effect we introduce a converter input voltage vector, described by formula (6), to take over the control process [4]:

$$\mathbf{U}_p = \mathbf{E} - j\omega_1 L \mathbf{I}_{\mathbf{xy}}, \tag{6}$$

where: $\mathbf{U}_p$ – converter input voltage vector.

To adjust the control in relation to $\mathbf{U}_p$, the vector of virtual flux should be turned by angle δ and the current errors in the *xy* rotating reference frame by angle $-\delta$ respectively. Finally, the control structure of the DPC $3\times2-\delta$ takes the shape introduced in Figure 7.

DPC $5\times2-\delta$

The DPC $5\times2-\delta$ [4] algorithm is, in fact, the DPC $3\times2-\delta$ method supplemented by the use of the three-level converter capabilities. The schematic diagram of the method is shown in Figure 8.

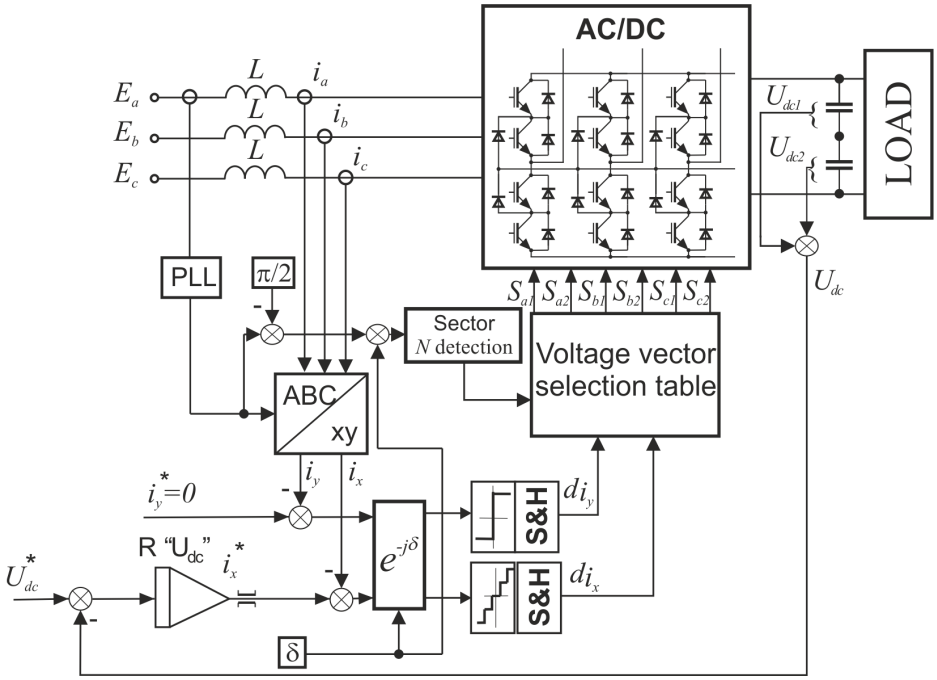

Fig. 8. Schematic diagram of DPC $5\times2-\delta$ method

www.czasopisma.pan.pl PAN POLSKA AKADEMIA NAUK www.journals.pan.pl

Due to an increased number of available voltage vectors (Fig. 2a), the number of current comparator levels in axis x rose from 3 to 5. Additional current comparator levels are used to control current by means of short current and long current derivatives in the static and dynamic state respectively.

Table 2. Voltage vector selection table for DPC 5×2–δ metod

		$N=1$	$N=2$	$N=3$	$N=4$	$N=5$	$N=6$
		number of voltage vector n					
$d_y=1$	$d_x=2$	25	26	21	22	23	24
	$d_x=1$	7.13	8.14	3.9	4.10	5.11	6.12
	$d_x=0$	6.12	7.13	8.14	3.9	4.10	5.11
	$d_x=-1$	5.11	6.12	7.13	8.14	3.9	4.10
	$d_x=-2$	23	24	25	26	21	22
$d_y=-1$	$d_x=2$	26	21	22	23	24	25
	$d_x=1$	8.14	3.9	4.10	5.11	6.12	7.13
	$d_x=0$	3.9	4.10	5.11	6.12	7.13	8.14
	$d_x=-1$	4.10	5.11	6.12	7.13	8.14	3.9
	$d_x=-2$	22	23	24	25	26	21

DPC-3Am

The current comparators used in the methods described above divide the error area in an unfavourable way. This is easy to prove for the case showed in Figure 9a where the impact of $\mathbf{U}_d[0]$ and $\mathbf{U}_d[2]$ voltage vectors is not equivalent. As can be noted the selection of $\mathbf{U}_d[2]$ vector is more advantageous because after T_p time, $\mathbf{U}_d[2]$ vector shifts the error vector (7) closer to zero ($|\boldsymbol{\varepsilon}_2|<|\boldsymbol{\varepsilon}_1|$).

$$\boldsymbol{\varepsilon} = \varepsilon_x + j\varepsilon_y, \tag{7}$$

where: ε_x, ε_y – components of error vector in xy rotating reference frame.

The determination of the optimal boundary requires a delimitation of such a dividing line, where the impact of the two adjacent voltage vectors is equivalent ($|\boldsymbol{\varepsilon}_2| = |\boldsymbol{\varepsilon}_1|$). The division in error area for DPC-3Am method is shown in Figure 9b. In this case, after time T_p the lengths of error vectors are equal ($|\boldsymbol{\varepsilon}_2| = |\boldsymbol{\varepsilon}_1|$) for both $\mathbf{U}_d[0]$ and $\mathbf{U}_d[2]$ voltage vectors. That means that the selection between either vectors is equivalent.

It was shown [8] that the boundaries of an optimum error distribution area are made up of three half-lines of common origin, and turned against each other by 120º. The boundaries of error distribution area are shifted by angle δ with respect to the x-axis and the common origin of boundaries is shifted from the origin of the coordinate system by $\mathbf{W}_i$ vector (Fig. 9c).

Vector $\mathbf{W}_i$ is related to vector $\mathbf{W}$ by formula (8) [8]:

$$\mathbf{W}_i = \frac{\mathbf{W}}{\mathrm{L}} T_p, \tag{8}$$

where: T_p – sample time.

Vector $\mathbf{W}$ is calculated using formula (9) as shown in Figure 9c:

www.czasopisma.pan.pl PAN POLSKA AKADEMIA NAUK www.journals.pan.pl

$$\mathbf{W} = \mathbf{U}_p - \mathbf{S}. \tag{9}$$

Where **S** is the vector of the centre of the equilateral triangle built of three voltage vectors characterized by the shortest current derivatives in actual *N* sector. Vector **S** can be calculated using formula (10) [4]:

$$\mathbf{S} = \frac{1}{3}(\mathbf{W_{b1}} e^{j\delta} + \mathbf{W_{b2}} e^{j\delta}), \tag{10}$$

where: $\mathbf{W}_{b1}$, $\mathbf{W}_{b2}$ – voltage vectors $\mathbf{U}_d[n]$ used in actual *N* sector (Fig. 9d).

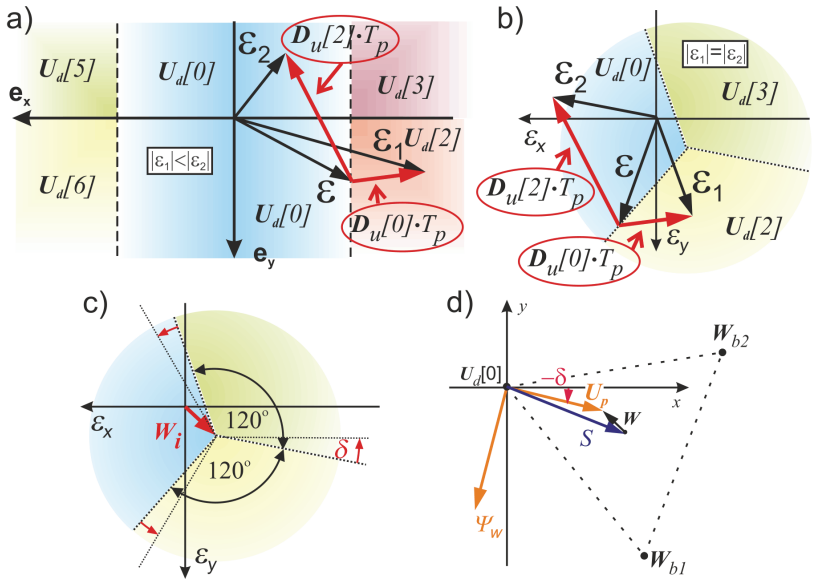

Fig. 9. Error distribution area in sector $N = 1$ for both DPC 3×2 (a) and DPC-3Am (b) (c) methods as well as graphical representation of the vector of the center of triangle **S** and vector **W** for DPC-3Am method (d)

In DPC-3Am method the real value of current is compared to set values of current in both axes of rotating reference frame. Error vector $\boldsymbol{\varepsilon}$ is created from ε_x, ε_y and subsequently according to formula (11), i.e. vector $\mathbf{W}_i$ is subtracted from error vector $\boldsymbol{\varepsilon}$ and then turned by angle $-\delta$ [8]:

$$\varepsilon'' = (\varepsilon - \mathbf{W}_i)\cdot e^{-j\delta} = |\varepsilon''|\cdot e^{j\varphi_{\varepsilon''}} \tag{11}$$

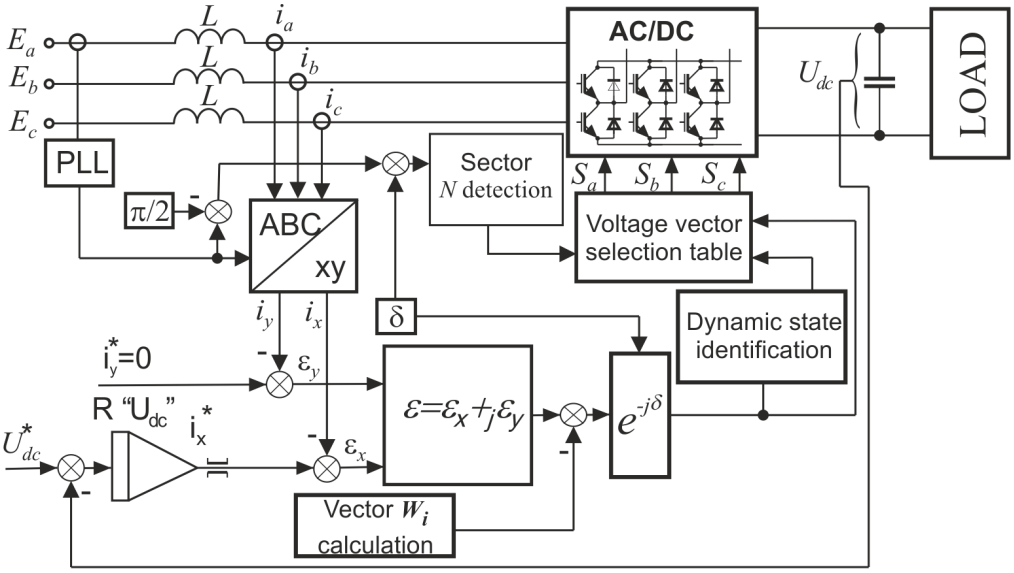

Fig. 10. Schematic diagram of DPC-3Am method

Table 3. Voltage vector selection table for DPC-3Am method

	$N=1$	$N=2$	$N=3$	$N=4$	$N=5$	$N=6$
	number of voltage vector n					
$\varphi_{\varepsilon''} \in \left(-\pi,-\frac{\pi}{3}\right)$	3	4	5	6	1	2
$\varphi_{\varepsilon''} \in \left(\frac{-\pi}{3},\frac{\pi}{3}\right)$	0.7	0.7	0.7	0.7	0.7	0.7
$\varphi_{\varepsilon''} \in \left(\frac{\pi}{3},\pi\right)$	2	3	4	5	6	1

DPC-3L-3Am

The DPC-3L-3Am [4] (Direct Power Control – 3 Level – 3 Area with modification) method is a modification of DPC-3Am method making use of an increased number of active vectors of three-level converter.

In order to reduce switching frequency in static states, converter voltage vectors corresponding to short current derivatives should be used. It was shown in [7] that the above voltage vectors in the two-level converter form an equilateral triangle (Fig. 11a) in each N sector, whereas in the three-level converter each N sector can be divided into four similar deltas (Fig. 11b). Optimal error areas for each of the equilateral triangles can be determined in an analogous way to DPC-3Am method.

www.czasopisma.pan.pl PAN POLSKA AKADEMIA NAUK www.journals.pan.pl

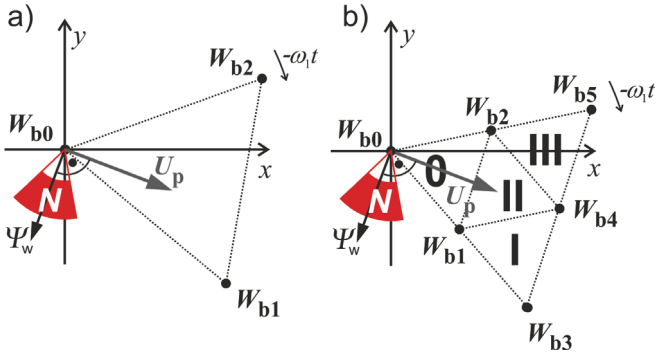

Fig. 11. Coverter voltage vectors made up of equilateral triangles in two- (DPC-3Am)(a) and tree-level (DPC-3L-3Am) (b) converters

Vector $\mathbf{U}_{sec1}$ and angle $\varphi_{U\text{sec}2}$ (Fig. 12) are introduced in order to choose a suitable triangle. These variables are defined by equations (12) and (13):

$$\mathbf{U}_{\text{sec}1} = \mathbf{W}_{b4} = |\mathbf{U}_{\text{sec}1}| \cdot e^{j\varphi_{\mathbf{U}\text{sec}1}}, \tag{12}$$

$$\varphi_{U_{\text{sec}2}} = \arcsin\left(\frac{|\mathbf{U}_p|}{|\mathbf{U}_{\text{sec}1} - \mathbf{U}_p|} \sin\left(\varphi_{U\text{sec}1} - \varphi_{U_p}\right) \right). \tag{13}$$

If the projection of vector $\mathbf{U}_p$ on $\mathbf{U}_{sec1}$ is shorter than half of vector's $\mathbf{U}_{sec1}$ length, then $\mathbf{U}_p$ vector is located inside triangle 0 (Fig. 12). This state is described by inequality (14):

$$\left| \frac{\mathbf{U}_{\text{sec}1}}{2} \right| > |\mathbf{U}_p| \cdot \cos(\varphi_{\text{sec}1} - \delta). \tag{14}$$

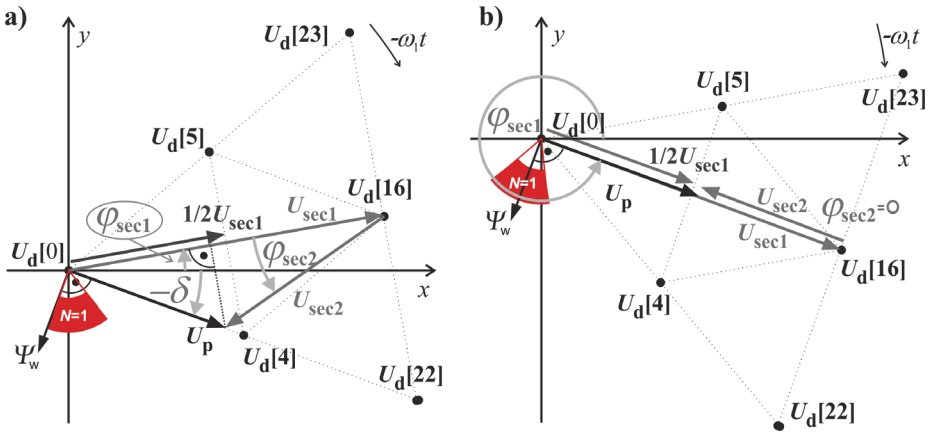

Fig. 12. Graphic interpretation of voltage vectors $\mathbf{U}_{sec1}$, and $\mathbf{U}_{sec2}$, as well as angle $\varphi_{U\text{sec}2}$ for both situations (when virtual flux vector is in the beginning (a) and in the middle (b) of sector $N = 1$)

In the case when inequality (14) is faulty, the choice of triangle is dependent on $\varphi_{U\text{sec}2}$ angle, according to Table 4.

Table 4. Triangle selection table

$\varphi_{U\text{sec}2} \in \left(\frac{\pi}{6}, \frac{\pi}{2}\right)$	triangle I
$\varphi_{U\text{sec}2} \in \left(-\frac{\pi}{6}, \frac{\pi}{6}\right)$	triangle II
$\varphi_{U\text{sec}2} \in \left(-\frac{\pi}{2}, -\frac{\pi}{6}\right)$	triangle III

Optimal error areas (Fig. 13) for each of the equilateral triangles can be determined in an analogous way to DPC-3Am method.

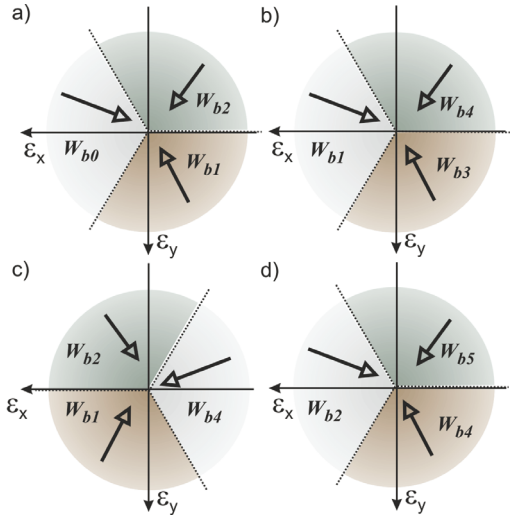

Fig. 13. Error distribution areas for triangles 0 (a), I (b), II (c) and III (d) in $N = 1$ sector

As shown in Figure 13 the boundaries of error distribution area for 0, I and III triangles are identical. In order to present error area distribution for triangle II in similar way the sign of component x should be changed into the opposite one (15) (Fig. 14).

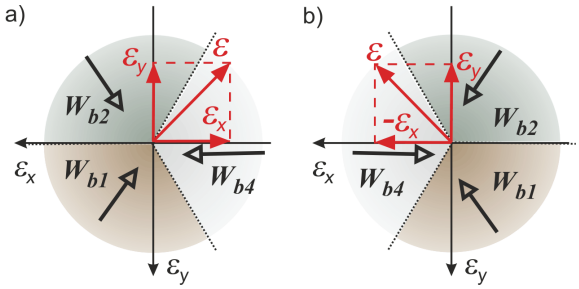

Fig. 14. Error distribution area in triangle II before (a) and after (b) the change of the sign of component *x* of the error vector

www.czasopisma.pan.pl PAN POLSKA AKADEMIA NAUK www.journals.pan.pl

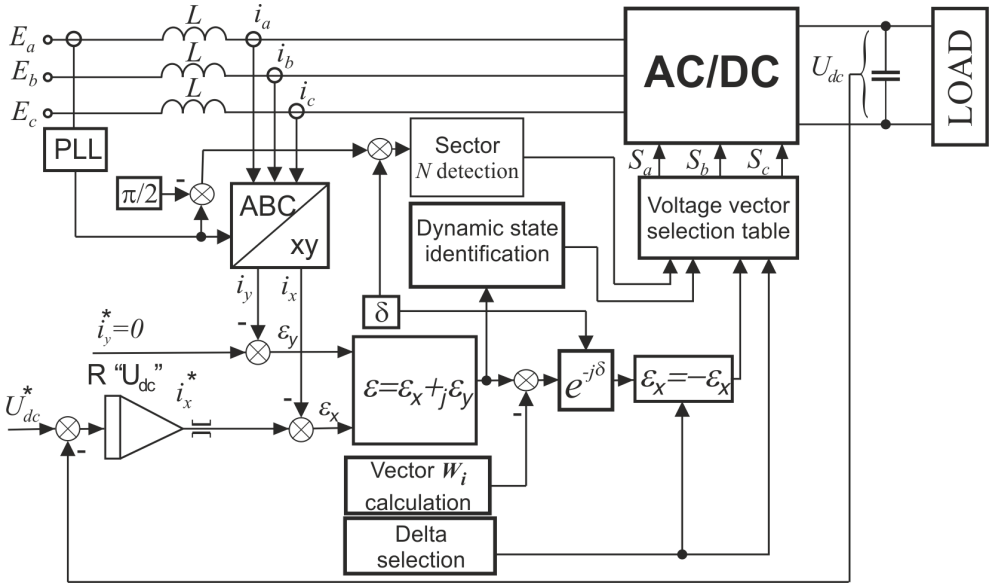

Fig. 15. Schematic diagram of DPC-3L-3Am method

In DPC-3L-3Am method the real value of current is compared to set values of current in both axes of rotating reference frames. Error vector ε is created out from errors ε_x, ε_y and subsequently transformed in agreement with formula (15), i.e. vector $\mathbf{W}_i$ is subtracted from error vector $\boldsymbol{\varepsilon}$ and then turned by angle $-\delta$. In the case when converter input voltage vector $\mathbf{U}_p$ is in triangle II the sign of component x is changed into the opposite one [9]:

$$\left|\varepsilon''\right| \cdot e^{j\varphi_\varepsilon} = \begin{cases} (\varepsilon_x + j\varepsilon_y - \mathbf{W_i}) \cdot e^{-j\delta}, \text{ for triangles } 0, \text{I}, \text{III}, \\ (-\varepsilon_x + j\varepsilon_y - \mathbf{W_i}) \cdot e^{-j\delta}, \text{ for triangle II}. \end{cases} \tag{15}$$

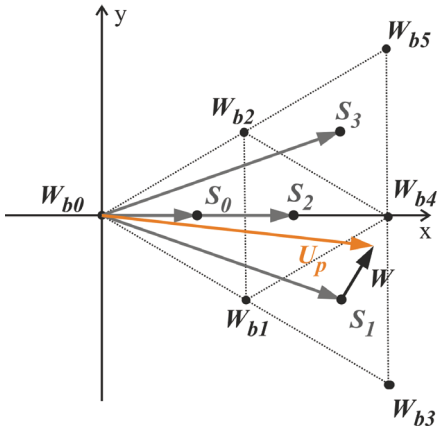

Fig. 16. Graphic interpretation of the vector **W** in DPC-3L-3Am method

www.czasopisma.pan.pl PAN POLSKA AKADEMIA NAUK www.journals.pan.pl

Vector **S** in DPC-3L-3Am method is dependent on delta where the converter input voltage vector $\mathbf{U}_p$ is currently used. The vector is described by formula (16) [9]:

$$\mathbf{S} = \begin{cases} \frac{1}{3}(\mathbf{W}_{b0} + \mathbf{W}_{b1} + \mathbf{W}_{b2}), \text{ for triangle } 0, \\ \frac{1}{3}(\mathbf{W}_{b1} + \mathbf{W}_{b3} + \mathbf{W}_{b4}), \text{ for triangle I}, \\ \frac{1}{3}(\mathbf{W}_{b1} + \mathbf{W}_{b2} + \mathbf{W}_{b4}), \text{ for triangle II}, \\ \frac{1}{3}(\mathbf{W}_{b2} + \mathbf{W}_{b4} + \mathbf{W}_{b5}), \text{ for triangle III}. \end{cases} \tag{16}$$

Table 5. Voltage vector selection table for DPC-3L-3Am method

		$N = 1$	$N = 2$	$N = 3$	$N = 4$	$N = 5$	$N = 6$
φ_ε	triangle	number of converter voltage vector n					
$\left(-\pi; -\frac{\pi}{3}\right)$	0	5, 11	6, 12	7, 13	8, 14	3, 9	4, 10
	I	16	17	18	19	20	15
	II	5, 11	6, 12	7, 13	8, 14	3, 9	4, 10
	III	23	24	25	26	21	22
$\left(-\frac{\pi}{3}, \frac{\pi}{3}\right)$	0	0, 1, 2	0, 1, 2	0, 1, 2	0, 1, 2	0, 1, 2	0, 1, 2
	I	4, 10	5, 11	6, 12	7, 13	8, 14	3, 9
	II	16	17	18	19	20	15
	III	5, 11	6, 12	7, 13	8, 14	3, 9	4, 10
$\left(\frac{\pi}{3}, \pi\right)$	0	4, 10	5, 11	6, 12	7, 13	8, 14	3, 9
	I	22	23	24	25	26	21
	II	4, 10	5, 11	6, 12	7, 13	8, 14	3, 9
	III	16	17	18	19	20	15

4. Experimental results

Laboratory setup used for experimental investigations of the described methods consisted of a three level AC/DC converter connected to the grid and a resistant load. The converter was controlled by DSP digital control system based on ADSP-21363 32-bit floating-point SHARC processor.

The experimental investigations were performed for 650 V DC link voltage, and three values of current i.e. 8, 16 and 24 A. The inductor inductance value was 20 mH. The basis for comparing the methods in static states was the similarity of phase current total harmonic

www.czasopisma.pan.pl PAN POLSKA AKADEMIA NAUK www.journals.pan.pl

distortion (THD). The values determined in the experiments performed for DPC 3×2 method at 40 μs sample time were adopted as reference values.

It should be emphasized here that a three-level converter was used in both DPC 3×2-δ and DPC-3L-3Am methods. The switchings of the semiconductors in three-level converters occur at twice lower voltage than in two-level ones. As a result, switching energy losses in three-level converters operating at the same switching frequency is twice smaller. Taking the above into account and the fact that tree-level converters use a double number of switching devices, the comparison of described methods using average switching frequency for one switching device is most convenient.

Table 6. Experimental results

	I^*_x	*THD*	*f*	T_p
	A	%	kHz	μs
DPC-3×2	8	7.47	7.42	40
DPC-3×2-δ		7.67	7.24	40
DPC-3Am		7.47	3.62	80
DPC-5×2-δ		7.40	3.46	80
DPC-3L-3Am		7.40	1.27	160
DPC-3×2	16	4.03	7.23	40
DPC-3×2-δ		4.10	6.8	40
DPC-3Am		3.97	3.41	80
DPC-3×2-δ		4.03	3.53	80
DPC-3L-3Am		4.03	1.26	160
DPC-3×2	24	3.03	6.78	40
DPC-3×2-δ		3.07	6.42	40
DPC-3Am		3.03	3.10	80
DPC-5×2-δ		3.00	3.48	80
DPC-3L-3Am		3.03	1.17	150

Basing on the experimental results (see Tab. 4), we can state that the DPC-3L-3Am method is characterized by the lowest switching frequency. Moreover, we can say that the DPC-3Am method is characterized by the lowest switching frequency in the group of methods dedicated to two-level converters.

As can be seen in Table 4, the use of the DPC-3L-3Am method reduces the number of converter switchings by more than 82% compared with the DPC 3×2 method, and by more than 62% compared with the DPC 3×2-δ method.

The use of the DPC-3Am method will cause a decrease of the number of switchings by more than 51% compared to the DPC 3×2 method.

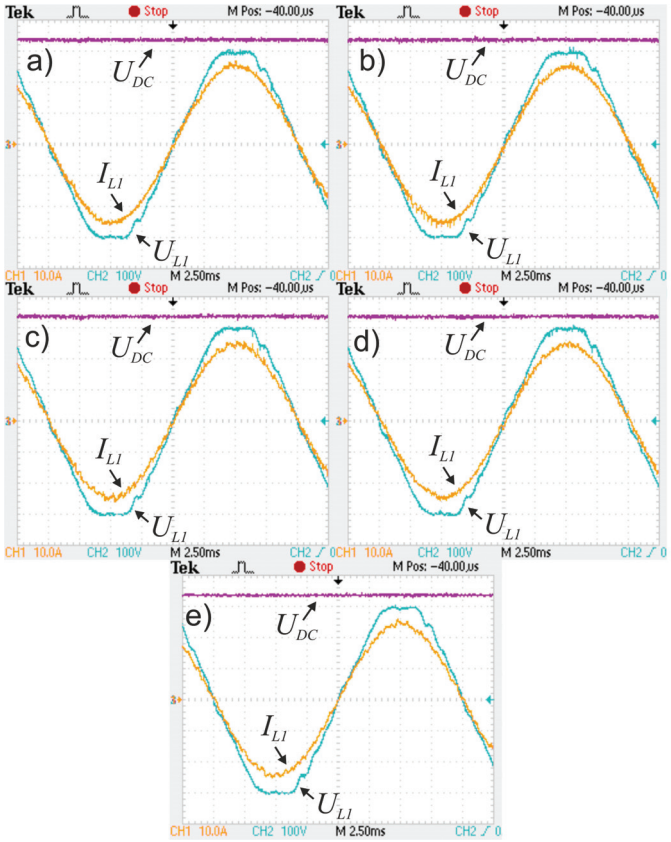

Fig. 17. Time courses of phase current, phase voltage and DC voltage for set value of current $I^*_x \approx 24$ A for methods: DPC 3×2 (a), DPC 3×2-δ (b), DPC-3Am (c), DPC 3×2-δ (d) DPC-3L-3Am (e)

5. Conclusion

The results of experimental studies have shown that using new modified methods of Direct Power Control in two- as well as three-level converters is more beneficial. In static states, with similar values of current deformations, it is possible to control converters with lower average switching frequency (thus reducing switching energy losses) and with longer sample time than in DPC methods for the same converter configuration.

The most advantageous control method for two-level converters has been proved to be the DPC-3Am method. This method reduces the number of switchings by approximately 51-54% compared with the DPC 3×2 method.

The best results of control three-level converter have proved DPC-3L-3Am method. This method reduces the number of switchings by approximately 82% compared with the DPC 3×2 method, by approximately 63-66% compared with the DPC-5×2-δ method, and by approximately 62-65% compared with the DPC-3Am method.

www.czasopisma.pan.pl PAN POLSKA AKADEMIA NAUK www.journals.pan.pl

Acknowledgement

The work was supported by research project W/WE/12/2011

References

[1] Vazquez S., Sanchez J.A., Carrasco J.M. et al., *A Model-Based Direct Power Control for Three-Phase Power Converters.* IEEE Trans. on Industrial Electron. 55 (4): 1647-1657 (2008).

[2] Malinowski M., Kazmierkowski M.P., Trzynadlowski A.M., *A comparative study of control techniques for PWM rectifiers in AC adjustable speed drives.* IEEE Trans. Power Electron. 18 (6), 1390-1396 (2003).

[3] Rueckert B., Hofmann W., *Common Mode Voltage Minimized Direct Power Control of the Grid Side Connected Converter in Doubly Fed Induction Generators.* International Symposium on Power Electronics, Electrical Drives, Automation and Motion SPEEDAM 2008, Italy, Ischia, pp. 1455-1459 (2008).

[4] Kulikowski K., Sikorski A., *Comparison of new DPC methods for two-and three-level AC/DC converters.* Przegląd Elektrotechniczny 87(1): 56-61 (2011).

[5] Kulikowski K., Sikorski A., *Regulacja mocy trójpoziomowego przekształtnika AC/DC współpracującego z siecią.* (*Power control of three-level AC/DC inverter with the cooperation of network*). Przegląd Elektrotechniczny 86(2): 179-184 (2010), (in Polish).

[6] Sikorski A., *Problemy minimalizacji strat łączeniowych w przekształtnikach AC/DC/AC – PWM zasilających maszynę indukcyjną.* Wydział Wydawnictw i Poligrafii (1998), (in Polish).

[7] A. Sikorski, *Bezpośrednia regulacja momentu i strumienia silnika indukcyjnego.* Oficyna Wydawnicza Politechniki Białostockiej (2009), (in Polish).

[8] Kulikowski K., Sikorski A., *Sterowanie przekształtnika AC/DC współpracującego z siecią metodą DPC-3A.* (*DPC-3A control method of AC/DC converter connected to AC grid*) Przegląd Elektrotechniczny 86(4): 130-133 (2010), (in Polish).